JPET Fast Forward. Published on October 3, 2019 as DOI: 10.1124/jpet.119.261040
This article has not been copyedited and formatted. The final version may differ from this version.

Title Page

A novel small molecule inhibits tumor growth and synergizes effects of enzalutamide on prostate cancer

Authors and Affiliations

Jiongjia Cheng*, Stephanie Moore, Jorge Gomez-Galeno, Dong-Hoon Lee, Karl J. Okolotowicz and John R. Cashman

Human BioMolecular Research Institute and ChemRegen, Inc., San Diego, CA, 92121, USA

JPET Fast Forward. Published on October 3, 2019 as DOI: 10.1124/jpet.119.261040
This article has not been copyedited and formatted. The final version may differ from this version.

Running Title Page

Running Title: Potent inhibition of prostate cancer

Corresponding author: Jiongjia Cheng, Ph.D., Human BioMolecular Research Institute, 5310 Eastgate Mall, San Diego, CA, 92121, USA. Phone: 858-458-9305, Fax: 858-458-9311. E-mail: jcheng@hbri.org.

Number of text pages: 35

Number of tables: 3

Number of figures: 5

Number of references: 40

Number of words in Abstract: 196

Number of words in Introduction: 618

Number of words in Discussion: 1150

Keywords:

prostate cancer; castrate-resistant prostate cancer; enzalutamide; drug synergy; xenograft model

JPET Fast Forward. Published on October 3, 2019 as DOI: 10.1124/jpet.119.261040
This article has not been copyedited and formatted. The final version may differ from this version.

Abbreviations:

Abiraterone (Abi); Androgen-dependent (AD); Androgen-depletion independent (ADI); Absorption, Distribution, Metabolism, and Excretion (ADME); Androgen-independent (AI); Androgen receptor (AR); Castrate-resistant prostate cancer (CRPCa); Combination index (CI); Enzalutamide (Enza); Food and Drug Administration (FDA); Half maximal effective concentration (EC_{50}); Half maximal inhibitory concentration (IC_{50}); Institutional Animal Care and Use Committee (IACUC); Intraperitoneal(ly) (i.p.); Mitochondrial Membrane Potential ($\Delta\Psi_m$); Outer mitochondrial membrane (OMM); Prostate cancer (PCa); Prostate Cancer San Diego 1 (PCSD1); Room temperature (r.t.); Serum Glutamic Oxaloacetic Transaminase/Aspartate Aminotransferase (SGOT (AST)); Serum Glutamic Pyruvic Transaminase/Alanine Aminotransferase (SGPT (ALT)); Standard deviation (SD); Standard error of mean (SEM); Tetramethylrhodamine, ethyl ester (TMRE)

Recommended section: Drug Discovery and Translational Medicine

Abstract

Prostate cancer (PCa) is the second leading cause of cancer-related death for men in the United States. About 35% of PCa recurs and is often transformed to castrate-resistant PCa (CRPCa), the most deadly and aggressive form of PCa. However, the standard-of-care treatment for CRPCa (e.g., enzalutamide with abiraterone) usually has limited efficacy. Herein, we report a novel molecule (i.e., PAWI-2) that inhibits cellular proliferation of androgen-sensitive (i.e., LNCaP) and androgen-insensitive (i.e., PC-3) cells. In vivo studies in a PC-3 xenograft model showed that PAWI-2 (20 mg/kg/day, 21 days, i.p.) inhibited tumor growth by 49% compared to vehicle-treated mice. PAWI-2 synergized currently clinically used enzalutamide in in vitro inhibition of PCa cell viability and re-sensitized inhibition of in vivo PC-3 tumor growth. Compared to vehicle-treated mice, PC-3 xenograft studies also showed that PAWI-2 (20 mg/kg/day, 21 days, i.p.) and enzalutamide (5 mg/kg/day, 21 days, i.p.) inhibited tumor growth by 63%. Synergism was mainly controlled by the imbalance of pro-survival factors (i.e., Bcl-2, Bcl-xL, Mcl-1) and anti-survival factors (i.e., Bax, Bak) induced by affecting mitochondrial membrane potential/mitochondria dynamics. Thus, PAWI-2 utilizes a distinct mechanism of action to inhibit PCa growth independently of androgen receptor signaling overcomes enzalutamide-resistant CRPCa.

Significance Statement

CRPCa is the most aggressive human PCa but standard chemotherapies for CRPCa are largely ineffective. PAWI-2 potently inhibits PCa proliferation in vitro and in vivo regardless of AR status and uses a distinct mechanism of action. PAWI-2 has greater utility in treating CRPCa than standard of care therapy. PAWI-2 possesses promising therapeutic potency in low-dose combination therapy with a clinically used drug (i.e., enzalutamide). This study describes a new approach to address the overarching challenge in clinical treatment of CRPCa.

JPET Fast Forward. Published on October 3, 2019 as DOI: 10.1124/jpet.119.261040
This article has not been copyedited and formatted. The final version may differ from this version.

Introduction

In the United States, prostate cancer (PCa) was the second leading cause of cancer-related fatalities for men and resulted in an estimated 29,430 deaths in 2018 (Siegel et al., 2018). PCa alone accounts for 19% of all cancer cases in men (Siegel et al., 2018). PCa is often initially responsive to anti-androgen hormone therapies and thus characterized as castration-sensitive PCa (Siegel et al., 2018). However, in 35% of patients, PCa recurs and is often transformed to castrate-resistant PCa (CRPCa), thus rendering hormone therapies ineffective (Gandhi et al., 2018; Howlader et al., 2019). This is an important distinction because the majority of PCa is non-lethal. The deadliest and most aggressive form of PCa is CRPCa that has a 40-month medium survival (Karantanos et al., 2013; Katzenwadel and Wolf, 2015). 80% of PCa patients develop bone metastasis and have a 25% five-year survival (Sturge et al., 2011). Today, most patients that die from PCa have CRPCa. However, effective drugs to treat CRPCa are lacking. Standard-of-care treatment options for CRPCa are limited to radiation or hormone therapy (e.g., enzalutamide) (Tran et al., 2009; Schalken and Fitzpatrick, 2016) or in combination with chemotherapy (e.g., docetaxel) (Mukherji et al., 2014).

Androgen receptor (AR), a steroid hormone receptor normally activated by androgens, plays an essential role in PCa development and progression (Gandhi et al., 2018). AR signaling is a critical survival pathway for PCa cells. Blockade of AR was shown to be an effective PCa therapeutic strategy (Tran et al., 2009; Schalken and Fitzpatrick, 2016). As one of the most effective AR-directed therapies, enzalutamide suppresses androgen action in PCa cells by inhibiting nuclear translocation, chromatin binding, and co-regulator binding of AR (Tran et al., 2009). This overcomes resistance to conventional anti-androgens (Azvolinsky, 2012). Use of enzalutamide increases overall survival 2.5-5 months (Scher et al., 2012; Dhingra et al., 2013).

JPET Fast Forward. Published on October 3, 2019 as DOI: 10.1124/jpet.119.261040
This article has not been copyedited and formatted. The final version may differ from this version.

However, survival benefits of enzalutamide were achieved in only about 50% of PCa patients treated (Scher et al., 2012; Dhingra et al., 2013). Patients that initially respond to enzalutamide eventually develop enzalutamide-resistance that results in a shorter survival interval due to acquired resistance (Katzenwadel and Wolf, 2015; Schalken and Fitzpatrick, 2016). Combination treatment of enzalutamide and abiraterone (i.e., a CYP17 enzyme inhibitor that blocks adrenal androgen biosynthesis (de Bono et al., 2011)) gave some improvement in PCa response. Clinical studies showed this multi-component therapy extended overall survival 4–5 months but many untoward gastric and hematologic side effects were observed (Gandhi et al., 2018). Moreover, most responding patients relapsed within 1-2 years with evidence of renewed AR activity (de Bono et al., 2011; Scher et al., 2012; Dhingra et al., 2013). Therefore, developing novel therapeutic approaches to overcome castrate-resistance are urgently needed in the treatment of CRPCa.

As previously reported, a first-in-class non-toxic anti-cancer compound (PAWI-2, **Fig. 1A**) was developed by targeting protein components of dysregulated signal transduction pathways in cancer (Cashman et al., 2013; Cheng et al., 2018; Okolotowicz et al., 2018; Cheng et al., 2019). PAWI-2 decreased cellular proliferation and induced apoptosis in several cancer cells (i.e., colon, breast and pancreatic cancer) (Cashman et al., 2013; Cheng et al., 2018; Okolotowicz et al., 2018; Cheng et al., 2019). PAWI-2 is a non-toxic DNA damage pathway inhibitor and activates mitochondrial-controlled p53-dependent apoptotic signaling (Cheng et al., 2018; Cheng et al., 2019). Herein, we report anti-cancer PAWI-2 (**Fig. 1A**) is an anti-PCa compound that works against androgen-sensitive PCa and androgen-insensitive CRPCa and also patient-derived bone niche PCa. PAWI-2 synergized currently clinically used enzalutamide in in vitro inhibition of PCa cell growth and also enhanced inhibition of tumor growth in a PC-3 xenograft model. PAWI-2

JPET Fast Forward. Published on October 3, 2019 as DOI: 10.1124/jpet.119.261040
This article has not been copyedited and formatted. The final version may differ from this version.

may afford more efficacious treatment with decreased side effects and also afford a molecule for both androgen-dependent and androgen-resistant PCa treatment.

Materials and Methods

Cell Lines

PC-3 (CRL-1435) and LNCaP (CRL-1740) PCa cells were purchased from American Type Culture Collection (ATCC). Prostate Cancer San Diego 1 (PCSD1) cells are a human prostate primary cancer cell freshly isolated from intra-femoral xenografts (generously provided by Dr. Christina Jamieson, UCSD) (Raheem et al., 2011; Godebu et al., 2014). Normal prostate epithelial cells (11220-hTERT) were kindly provided by Dr. John T. Isaacs (Graham et al., 2017) and grown in DermaLife keratinocyte serum-free medium (Lifeline Cell Technology). Commercial cell lines were grown according to ATCC recommendations and authenticated by short tandem repeat DNA profiling at ATCC. After thawing, cell lines were cultured at 37°C in a humidified 5% CO_2 atmosphere and routinely screened for mycoplasma contamination.

Compound synthesis

Synthesis and pharmaceutical properties of PAWI-2 (**Fig. 1A**) were reported (Cashman et al., 2013; Okolotowicz et al., 2018).

JPET Fast Forward. Published on October 3, 2019 as DOI: 10.1124/jpet.119.261040
This article has not been copyedited and formatted. The final version may differ from this version.

Cell viability and apoptosis

PCa cells were seeded and treated with vehicle (0.5% DMSO) or PAWI-2 (0.32-5000 nM). The effect of PAWI-2 on PCa (or 11220-hTERT) cell viability (72 hours) was determined by SYBRgreen (cellular DNA detection) fluorescence intensity (E_x/E_m = 495/535 nm) (Cheng et al., 2018; Cheng et al., 2019). Cellular proliferation was evaluated by determining the effect on cell viability at each day upon continuous 7-day treatment of PAWI-2. A similar protocol was used to test the synergy of PAWI-2 in the presence of enzalutamide and/or abiraterone. Chou-Talalay analysis was conducted with commercial software (ComboSyn) (Chou, 2010). Cell apoptosis was determined by a caspase-3/7 assay with Caspase-Glo 3/7 assay kit (Promega) (Cheng et al., 2018; Cheng et al., 2019).

Cell migration and invasion

PCa cells were pre-treated with vehicle, PAWI-2 (20-100 nM), enzalutamide (500 nM) or in combination, seeded in serum-free media on the upper side of a transwell chamber, either uncoated for a migration assay or coated with Matrigel (Corning) for invasion. Cells were allowed to migrate toward media containing 10% FBS for 24 hours. After the incubation period, cells on the lower side of the membrane were fixed, stained (0.5% crystal violet) and counted under a microscope (five random fields at 40× magnification).

TMRE Mitochondrial Membrane Potential

JPET Fast Forward. Published on October 3, 2019 as DOI: 10.1124/jpet.119.261040
This article has not been copyedited and formatted. The final version may differ from this version.

PCa cells were seeded and treated with vehicle, PAWI-2 (10-200 nM) or enzalutamide (500 nM) and/or abiraterone (3 μM) for 2-48 hours. Tetramethyl rhodamine, ethyl ester (TMRE) (250 nM) was added to cells in media and incubated for 30 min. The plate was depleted, washed, equilibrated in PBS/0.2% BSA (r.t. for 30 min) and fluorescence was read at E_x/E_m = 549/575 nm for calculation of %TMRE uptake compared to vehicle control.

Subcellular fractionation, Immunoblotting

Subcellular fractionation and immunoblotting experiments were carried out as previously described (Cheng et al., 2019). Briefly, PCa cells were seeded and treated with vehicle or PAWI-2 (i.e., 10-500 nM, 8-48 hours). Whole-cell extracts were obtained by lysis with RIPA buffer (**Supplementary Materials and Methods**) and subcellular fractionations were obtained and homogenized. Protein extracts were resolved by SDS-PAGE followed by Western blotting using antibodies specific for proteins of interest (**Supplementary Materials and Methods**). Densities of Western blot bands were quantified using ImageJ (NIH).

PC-3 xenograft

Animal work was conducted in accordance with the Guide for Care and Use of Laboratory Animals as adopted by NIH. Formal approval was obtained from the IACUC of HBRI. Athymic nude mice (6-week old males, Envigo, Placentia, CA) were anesthetized (xylazine/ketaved) and injected subcutaneously in the lower left flank with PC-3 cells (1 million log-phase cells in Matrigel matrix). Six days after cell implantation, animals with tumors were randomly assigned to

JPET Fast Forward. Published on October 3, 2019 as DOI: 10.1124/jpet.119.261040
This article has not been copyedited and formatted. The final version may differ from this version.

four groups and injected intraperitoneally in the right lower abdomen area with 0.1 ml of aqueous PEG (vehicle control), enzalutamide (5 mg/kg), PAWI-2 (20 mg/kg) or both PAWI-2 (20 mg/kg) and enzalutamide (5 mg/kg) formulated in aqueous PEG (final concentration, 20 % wt/vol), respectively. Mice were monitored and dosed daily for 21 days, and weighed once a week. Tumors were measured every 3-4 days by direct caliper measurements. At the end of the 26-day study, mice were killed and tumors were excised and weighed and immunobloted for analysis of select protein markers. Serum was obtained from blood samples for further analysis (IDEXX Laboratories).

Statistical analysis

IC_{50} and EC_{50} values were calculated using a nonlinear regression analysis (GraphPad Prism) of the mean and standard deviation (SD) or standard error of mean (SEM) of at least triplicate samples for each biological assay. One-way ANOVA tests (post Tukey's test) or *t*-tests were used to calculate statistical significance (GraphPad Prism) and a *P*-value less than 0.05 was considered statistically significant.

Results

Effect of PAWI-2 on PCa cell viability, proliferation, migration, invasion and apoptosis

JPET Fast Forward. Published on October 3, 2019 as DOI: 10.1124/jpet.119.261040
This article has not been copyedited and formatted. The final version may differ from this version.

PAWI-2 potently inhibited cell viability of PCa cells examined (i.e., IC_{50}s of 18, 14 nM for PC-3 and LNCap, respectively; 72 hours; **Table 1**, **Supplementary Fig. S1A**). PAWI-2 also showed dose-dependent inhibition of cellular proliferation in PCa cells upon continuous 7-day treatment (**Fig. 1B**). In a NCI-60 DTP Human Tumor Cell Line Screen (Shoemaker, 2006), PAWI-2 potently inhibited cell proliferation against two CRPCa cell lines (IC_{50}s of 34 and 46 nM for PC-3, DU-145, respectively). Inhibition by PAWI-2 was independent of AR response. Moreover, in human prostate primary cancer cells freshly isolated from intra-femoral xenografts (PCSD1) (Raheem et al., 2011; Godebu et al., 2014), PAWI-2 also potently inhibited cell viability (i.e., IC_{50} of 60 nM, **Table 1**). For comparison, PAWI-2 showed <20% inhibition (at 5 μM, 72 hours) on normal prostate epithelia cells (11220-hTERT) viability (**Supplementary Fig. S1A**). PAWI-2 was also not acutely cytotoxic or genotoxic as reported previously (Cheng et al., 2018).

PAWI-2 inhibited PCa cell migration and invasion in a dose-dependent manner (i.e., 20-100 nM, **Fig. 1C, D**). Compared to vehicle-treated PC-3 and LNCap cells, PAWI-2 (i.e., 100 nM, 24 hours) inhibited cell migration and invasion >2-fold. There was no significant inhibition on cell viability by PAWI-2 observed at this time point (i.e., 24 hours, **Supplementary Fig. S2**).

PAWI-2 potently activated apoptosis (i.e., activation of caspase-3/7 activity, **Fig. 1E**, **Supplementary Fig. S1B**) in LNCaP cells (PAWI-2, 35 nM; 8-fold to vehicle control at 48 hours). However, the effect was less apparent in PC-3 cells (PAWI-2, 100 nM; 2.5-fold, at 48 hours). Apoptosis was not observed in normal prostate epithelia cells (11220-hTERT, **Supplementary Fig. S1B**) treated with PAWI-2 (i.e., 0.32 nM to 5 μM; 24 hours). EC_{50} values for induction of apoptosis by PAWI-2 were consistent with IC_{50}s for inhibition of cell viability in LNCaP cells (EC_{50}, 11 nM versus IC_{50}, 14 nM) but 2-fold greater in PC-3 cells (EC_{50}, 35 nM versus IC_{50}, 18 nM) (**Table 1**). Stimulation of apoptosis by PAWI-2 was apparently dependent on the presence of

full-length p53 protein because apoptosis was somewhat less apparent for PAWI-2 in PC-3 cells with a p53 frameshift/premature stop mutation (van Bokhoven et al., 2003). This was consistent with previous reports of the effect of PAWI-2 in other cancer types (i.e., colon, pancreatic cancer) (Cheng et al., 2018; Okolotowicz et al., 2018; Cheng et al., 2019). P53-dependent apoptosis was observed by immunoblot results of PARP cleavage. PAWI-2 (i.e., 20-500 nM) potently induced cleavage of PARP (i.e., 48 hours, **Fig. 1F**) in LNCaP cells, but less potently in PC-3 cells. For example, EC_{50s} of PAWI-2 for PARP cleavage (i.e., 48, 12 nM in PC-3, LNCaP, respectively) were similar to EC_{50}s observed for *in vitro* caspase activation (i.e., 35, 11 nM for PC-3, LNCaP, respectively; **Table 1**).

Synergistic effect of PAWI-2 with enzalutamide in PCa cells

Compared to PAWI-2, enzalutamide (Enza), abiraterone (Abi) or a combination was less efficient at inhibiting in vitro cell viability in LNCaP cells (i.e., IC_{50}s >2 μM) and were not potent in PC-3 cells (**Table 2**). However, in the presence of a relatively low concentration of PAWI-2 (i.e., 2-8 nM), enzalutamide showed potent dose-response inhibition (**Supplementary Fig. S3**) on the cell viability of both PC-3 and LNCaP cells. Compared to enzalutamide treatment alone, in LNCaP cells, combination treatment (i.e., enzalutamide with PAWI-2) potently inhibited cell viability ~16-fold greater (IC_{50} 0.14 μM versus ~2.3 μM, **Table 2**). In the presence of PAWI-2, enzalutamide was observed to re-sensitize its inhibition on PC-3 cell viability (IC_{50} 1.4 μM, **Table 2**). However, combination of abiraterone with PAWI-2 was less effective because decreased IC_{50}s were not observed. Compared to enzalutamide alone (i.e., 500 nM) or enzalutamide and

JPET Fast Forward. Published on October 3, 2019 as DOI: 10.1124/jpet.119.261040
This article has not been copyedited and formatted. The final version may differ from this version.

abiraterone (i.e., 3 μM), a combination of enzalutamide with PAWI-2 (i.e., 10 nM) potently inhibited cell viability (i.e., $P<0.05$, **Fig. 2A**).

Based on Chou-Talalay synergism analysis (**Table 3**) (Chou, 2010), PAWI-2 synergized inhibition of cell viability by enzalutamide ("Enza + PAWI-2") against PC-3 and LNCaP cells and showed a low "combination index" value (i.e., CI values, 0.48-0.76 in PC-3 and 0.13-0.37 in LNCaP; **Table 3**). Synergism between abiraterone and PAWI-2 ("Abi + PAWI-2") was only observed in LNCaP cells (CI values, 0.7-0.74; **Table 3**). Antagonism (i.e., CI>1; **Table 3**) was observed between enzalutamide and abiraterone ("Enza + Abi") in either PC-3 or LNCaP cells. Combination treatment ("Enza + Abi + PAWI-2") showed less potent synergism compared to "Enza + PAWI-2".

Enhancement of inhibition of PCa cell migration and invasion was also observed in both PC-3 and LNCaP cells in the presence of enzalutamide with PAWI-2. Compared to enzalutamide alone in PC-3 and LNCaP cells, combination treatment ("Enza + PAWI-2") inhibited cell migration and invasion >3-fold greater (**Fig. 2B, C**). Meanwhile, there was also no significant inhibition of cell viability observed in this condition (**Supplementary Fig. S2**)

Mechanism studies. Synergy of the inhibitory effect of PAWI-2 on enzalutamide

Based on the effect of PAWI-2 on caspase 3/7 activity (i.e., PAWI-2, 35-100 nM potently induced apoptosis), PAWI-2 in combination with enzalutamide ("Enza + PAWI-2") was examined and compared to a combination of enzalutamide and abiraterone ("Enza + Abi", **Supplementary Fig. S4**, **Fig. 2D**). In LNCaP cells, PARP cleavage, a direct apoptotic marker was enhanced 1.6-

fold by PAWI-2 in combination with enzalutamide (**Supplementary Fig. S5**). However, this effect was not observed in PC-3 cells. Synergistic inhibition (against cell viability, cell migration and invasion; CI values < 1, **Table 3**; **Fig. 2A-C**) of enzalutamide with PAWI-2 was in part related to enhanced apoptosis. In PC-3 cells, apoptosis was induced by PAWI-2 alone (less potent than that in LNCaP cells) but combination treatment did not enhance apoptosis (**Fig. 2D**, **Supplementary Fig. S4**). Thus, induction of apoptosis may not be the sole mechanism of PAWI-2 to synergize the inhibitory effect of enzalutamide.

Enhancement of cell inhibition was p53-independent because synergism was observed in both PC-3 (*TP53* alleles: fs-sc/del; **Table 1**) and LNCaP (*TP53* alleles: WT/WT; **Table 1**) cells. Compared to PAWI-2 alone, neither total p53 (~3-fold) nor phospho(Ser15)-p53 activation (~20-fold) was enhanced by combination-treatment in LNCaP cells (**Supplementary Fig. S5**). ATR auto-phosphorylation in PC-3 or LNCaP cells was also observed in PAWI-2-treated cells, but was not enhanced in combination-treatment (**Supplementary Fig. S5**).

Synergism between enzalutamide and PAWI-2 ("Enza + PAWI-2") was associated with mitochondrial dysfunction observed by TMRE Mitochondrial Membrane Potential ($\Delta\Psi_m$) assessment (**Fig. 3A, B** and **Supplementary Fig. S6**). Changes in mitochondrial membrane potential in PCa cells treated with PAWI-2 or enzalutamide or a combination were quantified by %TMRE uptake. TMRE accumulates in active mitochondria (Ehrenberg et al., 1988). IC_{50}s of PAWI-2 to inactivate mitochondria or cause mitochondrial membrane potential loss (i.e., IC_{50}s of 46, 23 nM in PC-3, LNCaP cells, respectively; **Fig. 3A**) were similar to those values observed in other in vitro assays (**Table 1**). Compared to single or other compound combinations of enzalutamide and abiraterone, enzalutamide and PAWI-2 ("Enza, 500 nM + PAWI-2, 50-100 nM", 8 hours treatment) showed greatest inhibition of %TMRE uptake (20-25% greater, **Fig. 3B**).

JPET Fast Forward. Published on October 3, 2019 as DOI: 10.1124/jpet.119.261040
This article has not been copyedited and formatted. The final version may differ from this version.

Enhancement of the inhibition of TMRE uptake was associated with synergistic inhibition in combination treatment ("Enza + PAWI-2") against cell viability, cell migration and invasion (i.e., CI values < 1, **Table 3**; **Fig. 2A-C**).

We characterized the effect of enzalutamide, PAWI-2 or a combination of enzalutamide and PAWI-2 on mitochondrial-associated Bcl-2 family proteins (**Fig. 3C**) in comparison to other mitochondrial protein (i.e., matrix protein, HSP60; membrane proteins, TOM20, VDAC1). Pro-survival factors (i.e., Bcl-2, Bcl-xL, Mcl-1) were up-regulated by enzalutamide treatment in PCa cells. These proteins are either partially localized or exclusively integrated to outer mitochondrial membrane (OMM) to exert their functions (Wiedemann and Pfanner, 2017). PAWI-2 treatment alone caused mild degradation of OMM proteins. In the presence of enzalutamide, PAWI-2 attenuated Bcl-2, Bcl-xL, Mcl-1 protein levels back to normal. In contrast, anti-survival factors (i.e., Bax and Bak) were activated due to feedback control, the levels of which were unaffected or up-regulated by PAWI-2 or "Enza + PAWI-2" treatment. This facilitated incipient Cytochrome c release followed by cell growth inhibition. For comparison, the level of other mitochondrial localized proteins (i.e., HSP60, TOM20, VDAC1) were not affected by PAWI-2 (**Fig. 3C**).

Effect of PAWI-2 on tumor growth in a PC-3 xenograft model

Previous ADME, pharmacokinetics and pharmacodynamic studies showed PAWI-2 possessed sufficient chemical and metabolic stability, bioavailability and drug-like properties to examine its efficacy in vivo (Cheng et al., 2018; Okolotowicz et al., 2018; Cheng et al., 2019). Efficacy of PAWI-2 was examined either as a single agent or in combination with enzalutamide in a PC-3 xenograft animal model. Throughout the 26-day study, there was no statistically

significant difference in the animal weight of the animals (**Fig. 4A**). None of the mice died prior to day 26 and all appeared normal and vigorous. Animals with tumors established (on day 6, average size, 63 mm^3) were treated with vehicle, enzalutamide (Enza), PAWI-2 or enzalutamide with PAWI-2 ("Enza + PAWI-2"). Compared to vehicle-treated animals, PAWI-2 (20 mg/kg/day, 21 consecutive days, i.p.) or enzalutamide (5 mg/kg/day, 21 consecutive days, i.p.) with PAWI-2 (20 mg/kg/day, 21 consecutive days, i.p.) decreased PC-3 tumor growth rate in mice (**Fig. 4B**). Vehicle-treated animals grew tumors to an average size of 332 mm^3 (i.e., 5.7-fold increase; **Fig. 4B**) at day 26. In comparison, treatment with enzalutamide alone, PAWI-2 alone or enzalutamide with PAWI-2 decreased tumor growth rate 15%, 29% and 63% respectively (relative to vehicle-treated group).

At the end of the study, excised tumor volumes and weights of PAWI-2-treated mice (20 mg/kg/day) were significantly lower than those of vehicle-treated mice (i.e., $P<0.05$; 50% and 49% relative to vehicle group, respectively; **Fig. 4C, D**). Excised tumor volumes and weights of "Enza + PAWI-2"- treated mice were significantly lower than those of enzalutamide alone-treated mice (i.e., $P<0.05$; 48% and 44% relative to Enza-treated group, respectively; **Fig. 4C, D**). For comparison, enzalutamide alone decreased tumor volume and tumor weight only to 95% and 73%, respectively, compared to vehicle-treated group. PAWI-2 significantly decreased PC-3 tumor growth in vivo and also re-sensitized the effect of enzalutamide inhibition. Combination treatment ("Enza + PAWI-2") inhibited tumor weight (additional 18% decrease) greater than the PAWI-2 alone-treated group (**Fig. 4D**).

There was no significant difference in serum clinical parameters between the groups except the value of SGOT (AST) in enzalutamide alone-treated mice (**Supplementary Table S1**). In mice with combination treatment ("Enza + PAWI-2"), PAWI-2 decreased SGPT (ALT), SGOT (AST)

and glucose levels induced by enzalutamide treatment. Serum clinical data suggested that treatment of animals with PAWI-2 (20 mg/kg/day, 21 days, i.p.) showed normal liver, kidney or blood parameters. Moreover, PAWI-2 in combination with enzalutamide may decrease some side effects of enzalutamide treatment, like the most common hepatic effects with increased AST and ALT levels (Beer et al., 2018).

Immunoblot analysis of PC-3 tumors excised from xenografts

Tumors excised from animals upon termination of the xenograft study were analyzed for phosphorylated-ATM, Bcl-xL, Bak, Cytochrome c, or PARP proteins by immunoblots (**Fig. 5A, B**). DNA damage marker phosphor-ATM was not measurably affected across the groups. Pro-survival factor Bcl-xL was modestly up-regulated (1.4-fold) in the presence of enzalutamide but returned back to normal levels in "Enza + PAWI-2"-treated tumors. Compared to vehicle-treated mice, animals treated with PAWI-2 alone or a combination of "enzalutamide + PAWI-2" had on average 1.9-, 2.5-fold and 2.3-, 3.5-fold greater protein levels of Bak and Cytochrome c, respectively (**Fig. 5B**). The effect of PAWI-2 or "enzalutamide + PAWI-2" on protein markers in tumor tissue extract was consistent with in vitro PC-3 cell studies (**Fig. 1F**, **3C**, **Supplementary Fig. S5**). A similar effect on Bcl-xL, Bak and Cytochrome c was observed. The re-sensitizing effect of PAWI-2 on enzalutamide was mainly due to the imbalance of pro-survival factors (i.e., Bcl-xL) and anti-survival factors (i.e., Bak) induced by PAWI-2. In contrast, enzalutamide-only treated animals did not show any apparent increased levels of PARP cleavage, Bak or Cytochrome c. Compared to vehicle-treated mice, animals treated with PAWI-2 alone or "Enza + PAWI-2" had a 4-fold increase in PARP cleavage (**Fig. 5B**), indicative of induced apoptosis in these excised

tumors. However, PARP cleavage may not recapitulate the re-sensitized effect of enzalutamide because there was no enhancement of PARP cleavage upon comparison of "Enza + PAWI-2" to PAWI-2 alone.

Discussion

As previously reported (Cheng et al., 2018), PAWI-2 binds tubulin to cause tubulin destabilization (acetylated tubulin inhibition, IC_{50}s, 150-400 nM, 10-20 fold greater IC_{50s} than that observed in other in vitro pathways, IC_{50}s, 10-20 nM) (Cheng et al., 2018; Cheng et al., 2019). Even though PAWI-2 was found to destabilize microtubules in PCa cells in a similar manner to that observed in other cancer types (~2-fold inhibition of acetylated tubulin levels at 200 nM, **Supplementary Fig. S7A**), we favor a model that PAWI-2 causes partial inhibition of tubulin acetylation to "sense" and activate DNA-damage checkpoint and apoptosis in mitochondrial p53-dependent pathways in cancer (Cheng et al., 2018; Cheng et al., 2019). In addition, synergism of "enzalutamide + PAWI-2" was also not due to tubulin destabilization because inhibition of acetylated tubulin levels was not observed (**Supplemental Fig. S7B**) at the dose of PAWI-2 examined (i.e., 50-100 nM). Accordingly, we surmised that tubulin binding by PAWI-2 was not fully responsible for the pharmacological effects observed. The lack of stimulation of cell apoptosis by PAWI-2 in p53-deficient cells (Cheng et al., 2018; Cheng et al., 2019) showed that p53 played a significant role in the mechanism of action of PAWI-2 to induce cell apoptosis. P53-dependence of PAWI-2 was also observed in PCa cells (**Fig. 1E, F**) because apoptosis induced by PAWI-2 was significantly greater in LNCaP (WT p53) than that in PC-3 (similar to null p53

status). However, there was no apparent relationship observed between p53 mutation status and potency of PAWI-2 in inhibiting PCa cell viability (**Table 1**). There was also no apparent relationship between p53 status and synergism of PAWI-2 plus enzalutamide in PCa cells (**Fig. 2A-C**, **Table 3**). P53 activation may not be completely responsible for the potency of PAWI-2 in the presence of enzalutamide. Synergistic inhibition of PCa cell growth of PAWI-2 plus enzalutamide may be affected by more complex factors.

Expression of androgen receptor (AR) in PCa is heterogeneous. PCa cells are often classified as AR-expressing (i.e., AR^+, LNCaP) and AR low- or non-expressing (i.e., $AR^{-/lo}$, PC-3) cells (van Bokhoven et al., 2003). $AR^{-/lo}$ PCa cells are resistant to inhibition of cell viability for most commonly used therapy for androgen ablation (Katzenwadel and Wolf, 2015). For example, enzalutamide is an AR antagonist approved by the FDA in 2012 (Azvolinsky, 2012) and has been reported to be effective in the treatment of PCa. Most AR^+ PCa reportedly respond to androgen ablation therapies but often leads to androgen-depletion independent (ADI) status (Karantanos et al., 2013; Katzenwadel and Wolf, 2015). The currently incurable stage of PCa (i.e., CRPCa) remains a challenge to treat (Yang et al., 2009; Ni et al., 2013; Ritch and Cookson, 2016; Jernberg et al., 2017). Combination of enzalutamide with abiraterone is the most widespread first-line treatment for CRPCa (de Bono et al., 2011). In enzalutamide-sensitive LNCaP cells and enzalutamide-resistant PC-3 cells, "enzalutamide + PAWI-2" markedly increased the inhibition of PCa cell viability compared with enzalutamide alone or "enzalutamide + abiraterone" (**Table 2, 3**). Thus, PAWI-2 sensitized these cells to enzalutamide much more effectively than abiraterone. Greater than 90% of patients develop metastases from CRPCa that cause PCa-related deaths (Gandhi et al., 2018). Because cancer metastasis is a hallmark of malignancy in CRPCa, the finding that PAWI-2 inhibited PCa migration and invasion regardless of AR response status (**Fig. 1C, D**)

JPET Fast Forward. Published on October 3, 2019 as DOI: 10.1124/jpet.119.261040
This article has not been copyedited and formatted. The final version may differ from this version.

and also synergized/re-sensitized the effect of enzalutamide (**Fig. 2B, C**) is an important finding. Moreover, PAWI-2 also potently inhibited cell viability of bone metastatic CRPCa cells (PCSD1) (Raheem et al., 2011; Godebu et al., 2014). In summary, PAWI-2 is capable of interrupting highly invasive and metastatic properties of CRPCa.

Recent reports suggest that in addition to nuclear genomic signaling, AR may also participate in non-genomic signaling in PCa (i.e., control of mitochondrial function and retrograde signaling (Massie et al., 2011; Zarif and Miranti, 2016)). The mechanism of action of PAWI-2 was previously reported to be closely allied to mitochondrial function (Cheng et al., 2019). Herein, we showed that PAWI-2 causes the loss of mitochondrial membrane potential and affects mitochondrial membrane dynamics and import/translocation of proteins (e.g., degradation of several mitochondrial localized Bcl-2-like proteins; **Fig. 3C**). This effect was independent of AR status and also highly associated with synergism for "enzalutamide + PAWI-2". Other mitochondrial-localized proteins (i.e., HSP60, TOM20 or VDAC1) control general mitochondrial import machinery and mitochondrial respiration, the levels of which were not affected by PAWI-2. PAWI-2 may selectively affect the Bcl-2 family of proteins but not disrupt entire mitochondria integrity. There are other PCa drugs that reportedly interfere with mitochondrial membrane potential (e.g., docetaxel) (Mediavilla-Varela et al., 2009).

There are only a few medications or treatments approved to treat CRPCa, including docetaxel, cabazitaxel, abiraterone, enzalutamide and Radium-223 (Karantanos et al., 2013). Amongst these, enzalutamide is well-tolerated and has a favorable toxicity profile (Tran et al., 2009). However, enzalutamide treatment outcome remains modest. In a human CRPCa xenograft model (i.e., VCaP), enzalutamide (10 mg/kg/day; oral; 26 days) inhibited tumor growth 10% (Qiao et al., 2016). In another 22RV1-CRPCa model, mice treated with enzalutamide (20 mg/kg/day;

i.p.; 22 days) afforded an estimated 15% inhibition of tumor growth (Kong et al., 2018). For PC-3 xenograft models, cabazitaxel (5 mg/kg/week; i.p.; 8 weeks) showed 18% inhibition (Zhang et al., 2013) and docetaxel (5 mg/kg; b.i.w.; i.p.; 14 days) showed 35% inhibition (Mimeault et al., 2015) of tumor growth, respectively. These are lower levels of tumor growth inhibition compared to treatment with PAWI-2 (20 mg/kg/day, 49% inhibition) or "enzalutamide + PAWI-2" (63% inhibition, **Fig. 4**) with no observed toxicity (**Supplementary Fig. S1** and **Table S1**). Thus, the data herein show PAWI-2 is more efficacious than the most commonly used clinical treatment in an animal model of PCa. In addition, compared to other CRPCa drugs (Wishart et al., 2018), the excellent pharmaceutical properties of PAWI-2 (ADME properties and lack of toxicity, **Supplementary Table S2**) also distinguish this drug-like molecule from other PCa treatments. For example, acquired enzalutamide resistance is a hallmark of CRPCa (Li et al., 2018). Analysis of the PAINS alerts (Vidler et al., 2018) for PAWI-2 showed there was no apparent issues present for PAWI-2. Up-regulation of pro-survival factors (i.e., Bcl-2, Bcl-xL, Mcl-1) and The imbalance of pro-survival and anti-survival factors caused by PAWI-2 through affecting mitochondrial membrane potential/function may be a controlling mechanism in synergizing/re-sensitizing the effect of enzalutamide to overcome enzalutamide resistance.

In summary, PAWI-2 is a non-toxic, highly efficacious compound for PCa that showed considerable synergism with enzalutamide to decrease PCa cell viability, migration and invasion. PAWI-2 effectively inhibited tumor growth in a xenograft model of CRPCa cells (PC-3) as a single agent and also in combination with enzalutamide. Because of its novel mechanism of action, PAWI-2 has broad utility to treat more aggressive CRPCa and patient-derived bone niche CRPCa. PAWI-2 synergizes other PCa drugs and thus allows a lower dose, a decrease in toxicity and a re-sensitization of the effect of other PCa drugs (i.e., enzalutamide).

JPET Fast Forward. Published on October 3, 2019 as DOI: 10.1124/jpet.119.261040
This article has not been copyedited and formatted. The final version may differ from this version.

Acknowledgement

We thank Dr. Christina Jamieson of University of California, San Diego for the PCSD1 cells. We also thank Dr. John T. Isaacs at Sidney Kimmel Comprehensive Cancer Center (Johns Hopkins School of Medicine, Baltimore, Maryland) for the 11220-hTERT cells.

Authorship Contributions

Participated in research design: Cheng, Okolotowicz, Cashman

Conducted experiments: Cheng, Moore, Lee, Cashman

Contributed new reagents or analytic tools: Cheng, Gomez-Galeno, Okolotowicz, Cashman

Performed data analysis: Cheng, Moore, Lee

Wrote or contributed to the writing of the manuscript: Cheng, Gomez-Galeno, Cashman

References

Azvolinsky A (2012) FDA Approves Enzalutamide (Xtandi) for Late-Stage Prostate Cancer. CancerNetwork (https://www.cancernetwork.com/articles/fda-approves-enzalutamide-xtandi-late-stage-prostate-cancer), posted to the Cancer Network web site, September 4, 2012.

Beer TM, Chowdhury S, Saad F, Shore ND, Higano CS, Iversen P, Fizazi K, Miller K, Heidenreich A, Kim CS, Phung D, Barrus JK, Nikolayeva N, Krivoshik A, Waksman J and Tombal BF (2018) Hepatic effects assessed by review of safety data in enzalutamide castration-resistant prostate cancer (CRPC) trials. *Journal of Clinical Oncology* **36**:199.

Cashman JR, Mercola M, Schade D and Tsuda M (2013) Compounds for inhibition of cancer cell proliferation. *Google Patents*:US 13/748,770.

Cheng J, Dwyer M, Okolotowicz KJ, Mercola M and Cashman JR (2018) A Novel Inhibitor Targets Both Wnt Signaling and ATM/p53 in Colorectal Cancer. *Cancer Res* **78**:5072-5083.

Cheng J, Okolotowicz KJ, Ryan D, Mose E, Lowy AM and Cashman JR (2019) Inhibition of invasive pancreatic cancer: restoring cell apoptosis by activating mitochondrial p53. *Am J Cancer Res* **9**:390-405.

Chou TC (2010) Drug combination studies and their synergy quantification using the Chou-Talalay method. *Cancer Res* **70**:440-446.

de Bono JS, Logothetis CJ, Molina A, Fizazi K, North S, Chu L, Chi KN, Jones RJ, Goodman OB, Jr., Saad F, Staffurth JN, Mainwaring P, Harland S, Flaig TW, Hutson TE, Cheng T, Patterson H, Hainsworth JD, Ryan CJ, Sternberg CN, Ellard SL, Flechon A, Saleh M, Scholz M, Efstathiou E, Zivi A, Bianchini D, Loriot Y, Chieffo N, Kheoh T, Haqq CM,

Scher HI and Investigators C-A- (2011) Abiraterone and increased survival in metastatic prostate cancer. *N Engl J Med* **364**:1995-2005.

Dhingra R, Sharma T, Singh S, Sharma S, Tomar P, Malhotra M and Bhardwaj TR (2013) Enzalutamide: a novel anti-androgen with prolonged survival rate in CRPC patients. *Mini Rev Med Chem* **13**:1475-1486.

Ehrenberg B, Montana V, Wei MD, Wuskell JP and Loew LM (1988) Membrane potential can be determined in individual cells from the nernstian distribution of cationic dyes. *Biophys J* **53**:785-794.

Gandhi J, Afridi A, Vatsia S, Joshi G, Joshi G, Kaplan SA, Smith NL and Khan SA (2018) The molecular biology of prostate cancer: current understanding and clinical implications. *Prostate Cancer Prostatic Dis* **21**:22-36.

Godebu E, Muldong M, Strasner A, Wu CN, Park SC, Woo JR, Ma W, Liss MA, Hirata T, Raheem O, Cacalano NA, Kulidjian AA and Jamieson CA (2014) PCSD1, a new patient-derived model of bone metastatic prostate cancer, is castrate-resistant in the bone-niche. *J Transl Med* **12**:275.

Graham MK, Principessa L, Antony L, Meeker AK and Isaacs JT (2017) Low p16(INK4a) Expression in Early Passage Human Prostate Basal Epithelial Cells Enables Immortalization by Telomerase Expression Alone. *Prostate* **77**:374-384.

Howlader N, Noone AM, Krapcho M, Miller D, Brest A, Yu M, Ruhl J, Tatalovich Z, Mariotto A, Lewis DR, Chen HS, Feuer EJ and Cronin KA (2019) SEER Cancer Statistics Review, 1975-2016, National Cancer Institute. Bethesda, MD, https://seer.cancer.gov/csr/1975_2016/, based on November 2018 SEER data submission, posted to the SEER web site, April 2019.

Jernberg E, Bergh A and Wikstrom P (2017) Clinical relevance of androgen receptor alterations in prostate cancer. *Endocr Connect* **6**:R146-R161.

Karantanos T, Corn PG and Thompson TC (2013) Prostate cancer progression after androgen deprivation therapy: mechanisms of castrate resistance and novel therapeutic approaches. *Oncogene* **32**:5501-5511.

Katzenwadel A and Wolf P (2015) Androgen deprivation of prostate cancer: Leading to a therapeutic dead end. *Cancer Lett* **367**:12-17.

Kong Y, Cheng L, Mao F, Zhang Z, Zhang Y, Farah E, Bosler J, Bai Y, Ahmad N, Kuang S, Li L and Liu X (2018) Inhibition of cholesterol biosynthesis overcomes enzalutamide resistance in castration-resistant prostate cancer (CRPC). *J Biol Chem* **293**:14328-14341.

Li Q, Deng Q, Chao HP, Liu X, Lu Y, Lin K, Liu B, Tang GW, Zhang D, Tracz A, Jeter C, Rycaj K, Calhoun-Davis T, Huang J, Rubin MA, Beltran H, Shen J, Chatta G, Puzanov I, Mohler JL, Wang J, Zhao R, Kirk J, Chen X and Tang DG (2018) Linking prostate cancer cell AR heterogeneity to distinct castration and enzalutamide responses. *Nat Commun* **9**:3600.

Massie CE, Lynch A, Ramos-Montoya A, Boren J, Stark R, Fazli L, Warren A, Scott H, Madhu B, Sharma N, Bon H, Zecchini V, Smith DM, Denicola GM, Mathews N, Osborne M, Hadfield J, Macarthur S, Adryan B, Lyons SK, Brindle KM, Griffiths J, Gleave ME, Rennie PS, Neal DE and Mills IG (2011) The androgen receptor fuels prostate cancer by regulating central metabolism and biosynthesis. *EMBO J* **30**:2719-2733.

Mediavilla-Varela M, Pacheco FJ, Almaguel F, Perez J, Sahakian E, Daniels TR, Leoh LS, Padilla A, Wall NR, Lilly MB, De Leon M and Casiano CA (2009) Docetaxel-induced prostate cancer cell death involves concomitant activation of caspase and lysosomal pathways and is attenuated by LEDGF/p75. *Mol Cancer* **8**:68.

Mimeault M, Rachagani S, Muniyan S, Seshacharyulu P, Johansson SL, Datta K, Lin MF and Batra SK (2015) Inhibition of hedgehog signaling improves the anti-carcinogenic effects of docetaxel in prostate cancer. *Oncotarget* **6**:3887-3903.

Mukherji D, Omlin A, Pezaro C, Shamseddine A and de Bono J (2014) Metastatic castration-resistant prostate cancer (CRPC): preclinical and clinical evidence for the sequential use of novel therapeutics. *Cancer Metastasis Rev* **33**:555-566.

Ni L, Llewellyn R, Kesler CT, Kelley JB, Spencer A, Snow CJ, Shank L and Paschal BM (2013) Androgen induces a switch from cytoplasmic retention to nuclear import of the androgen receptor. *Mol Cell Biol* **33**:4766-4778.

Okolotowicz KJ, Dwyer M, Ryan D, Cheng J, Cashman EA, Moore S, Mercola M and Cashman JR (2018) Novel tertiary sulfonamides as potent anti-cancer agents. *Bioorg Med Chem* **26**:4441-4451.

Qiao Y, Feng FY, Wang Y, Cao X, Han S, Wilder-Romans K, Navone NM, Logothetis C, Taichman RS, Keller ET, Palapattu GS, Alva AS, Smith DC, Tomlins SA, Chinnaiyan AM and Morgan TM (2016) Mechanistic Support for Combined MET and AR Blockade in Castration-Resistant Prostate Cancer. *Neoplasia* **18**:1-9.

Raheem O, Kulidjian AA, Wu C, Jeong YB, Yamaguchi T, Smith KM, Goff D, Leu H, Morris SR, Cacalano NA, Masuda K, Jamieson CH, Kane CJ and Jamieson CA (2011) A novel patient-derived intra-femoral xenograft model of bone metastatic prostate cancer that recapitulates mixed osteolytic and osteoblastic lesions. *J Transl Med* **9**:185.

Ritch CR and Cookson MS (2016) Advances in the management of castration resistant prostate cancer. *BMJ* **355**:i4405.

Schalken J and Fitzpatrick JM (2016) Enzalutamide: targeting the androgen signalling pathway in metastatic castration-resistant prostate cancer. *BJU Int* **117**:215-225.

Scher HI, Fizazi K, Saad F, Taplin ME, Sternberg CN, Miller K, de Wit R, Mulders P, Chi KN, Shore ND, Armstrong AJ, Flaig TW, Flechon A, Mainwaring P, Fleming M, Hainsworth JD, Hirmand M, Selby B, Seely L, de Bono JS and Investigators A (2012) Increased survival with enzalutamide in prostate cancer after chemotherapy. *N Engl J Med* **367**:1187-1197.

Shoemaker RH (2006) The NCI60 human tumour cell line anticancer drug screen. *Nat Rev Cancer* **6**:813-823.

Siegel RL, Miller KD and Jemal A (2018) Cancer Statistics, 2018. *CA Cancer J Clin* **68**:7-30.

Sturge J, Caley MP and Waxman J (2011) Bone metastasis in prostate cancer: emerging therapeutic strategies. *Nat Rev Clin Oncol* **8**:357-368.

Tran C, Ouk S, Clegg NJ, Chen Y, Watson PA, Arora V, Wongvipat J, Smith-Jones PM, Yoo D, Kwon A, Wasielewska T, Welsbie D, Chen CD, Higano CS, Beer TM, Hung DT, Scher HI, Jung ME and Sawyers CL (2009) Development of a second-generation antiandrogen for treatment of advanced prostate cancer. *Science* **324**:787-790.

van Bokhoven A, Varella-Garcia M, Korch C, Johannes WU, Smith EE, Miller HL, Nordeen SK, Miller GJ and Lucia MS (2003) Molecular characterization of human prostate carcinoma cell lines. *Prostate* **57**:205-225.

Vidler LR, Watson IA, Margolis BJ, Cummins DJ and Brunavs M (2018) Investigating the Behavior of Published PAINS Alerts Using a Pharmaceutical Company Data Set. *ACS Med Chem Lett* **9**:792-796.

Wiedemann N and Pfanner N (2017) Mitochondrial Machineries for Protein Import and Assembly. *Annu Rev Biochem* **86**:685-714.

Wishart DS, Feunang YD, Guo AC, Lo EJ, Marcu A, Grant JR, Sajed T, Johnson D, Li C, Sayeeda Z, Assempour N, Iynkkaran I, Liu Y, Maciejewski A, Gale N, Wilson A, Chin L, Cummings R, Le D, Pon A, Knox C and Wilson M (2018) DrugBank 5.0: a major update to the DrugBank database for 2018 (https://www.drugbank.ca/). *Nucleic Acids Res* **46**:D1074-D1082.

Yang JC, Ok JH, Busby JE, Borowsky AD, Kung HJ and Evans CP (2009) Aberrant activation of androgen receptor in a new neuropeptide-autocrine model of androgen-insensitive prostate cancer. *Cancer Res* **69**:151-160.

Zarif JC and Miranti CK (2016) The importance of non-nuclear AR signaling in prostate cancer progression and therapeutic resistance. *Cell Signal* **28**:348-356.

Zhang S, Wang Y, Chen Z, Kim S, Iqbal S, Chi A, Ritenour C, Wang YA, Kucuk O and Wu D (2013) Genistein enhances the efficacy of cabazitaxel chemotherapy in metastatic castration-resistant prostate cancer cells. *Prostate* **73**:1681-1689.

Footnotes

This work was supported by Small Business Innovation Research Program Grant from US National Institutes of Health [R43CA203566; K. J. Okolotowicz]; Inception Award from California Institute for Regenerative Medicine [DISC1-10583; J.R. Cashman] and by funds from the Human BioMolecular Research Institute and ChemRegen, Inc.

Figure Legends

Figure 1. A) Structure of PAWI-2. **B**) Dose-dependent effect of PAWI-2 on inhibition of PCa cell proliferation, **C**) migration and **D**) invasion in PC-3 and LNCaP cells. **E**) Time-dependent activation of Caspase-3/7 activity by PAWI-2 determined by a Caspase-Glo 3/7 assay in PC-3 and LNCaP cells and **F**) Western blot analysis of PAWI-2 on PARP (full length) and cleaved PARP as determined from whole-cell extracts of PC-3 and LNCaP cells after treatment for 48 hours. Concentrations of PAWI-2 (10-500 nM) and treatment time used was as indicated: 0-7 days in **B**, 24 hours in **C**, **D**, 0-72 hours in **E** and 48 hours in **F**; Veh, vehicle control (0.5% DMSO). GAPDH was used as an internal control in **F**. Data are mean ± SD (n = 3); *P*-values were estimated by one-way ANOVA test in **B-F** (**P*<0.05, ***P*<0.01, ****P*<0.001).

Figure 2. Effect of PAWI-2 on inhibition of PCa cell **A**) viability, **B**) migration, **C**) invasion and **D**) activation of Caspase-3/7 in the presence of enzalutamide and/or abiraterone in PC-3 or LNCaP cells. Concentrations of enzalutamide and abiraterone treatment were 500 nM and 3 μM, respectively. The concentrations of PAWI-2 used in **A**: 10 nM; in **B**, **C**: 100 nM; in **D**: PC-3 (100 nM); LNCaP (20 nM). Treatment time was 72 hours in **A**, 24 hours in **B**, **C** and 48 hours in **D**. Veh, vehicle control (0.5% DMSO); Enza, enzalutamide; and Abi, abiraterone. Data are mean ± SD (n = 3); *P*-values were estimated by Student's *t*-test (**P*<0.05, ***P*<0.01, ****P*<0.001).

Figure 3. Effect of PAWI-2 on changes of mitochondrial membrane potential determined by **A, B**) TMRE assay and **C**) Western blotting of mitochondrial proteins in the presence of enzalutamide. **A**) Dose-dependent inhibition of %TMRE uptake by PAWI-2 (2-200 nM) and **B**) enhancement of enzalutamide on inhibition of %TMRE uptake by PAWI-2, **C**) Western blot analysis of Bcl-2, Bcl-

xL, Mcl-1, Bax, Bak, Cytochrome c (Cyt c), TOM20, VDAC1, HSP60 by PAWI-2 as determined from mitochondrial extracts of PC-3 and LNCaP cells. Concentrations of enzalutamide and abiraterone treatment were 500 nM and 3 µM, respectively. Concentrations of PAWI-2 were 100 nM in PC-3 and 50 nM in LNCaP. Treatment time was 24 hours in **A**, **C** and 8 hours in **B**. Veh, vehicle control (0.5% DMSO); Enza, enzalutamide; and Abi, abiraterone. GAPDH was used as an internal control in **C**. Data are mean ± SD (n = 3); *P*-values were estimated by one-way ANOVA test in **A** (***P<0.001) and by Student's *t*-test in **B** (*P<0.05, **P<0.01).

Figure 4. Effect of PAWI-2 on PC-3 tumor growth in a subcutaneous xenograft model in nu/nu mice. **A**) Average xenograft mice body weight (g); **B**) average tumor growth and **C**) tumor volume (mm^3) and **D**) weight (g) for excised tumors of animals treated with vehicle, enzalutamide, PAWI-2 or "enzalutamide + PAWI-2". Treatment was administered every day for 21 days starting on day 6 post PC-3 cell inoculation by intraperitoneal (i.p.) injection. Body weights were monitored once a week after inoculation. Tumors implanted in nu/nu mice were assessed by caliper measurements every 3-4 days after inoculation. Dose treatment: vehicle control (aqueous-PEG), n = 9; enzalutamide (5 mg/kg/day), n = 9; PAWI-2 (20 mg/kg/day), n = 9; or both enzalutamide (5 mg/kg/day) and PAWI-2 (20 mg/kg/day), n = 6; Enza, enzalutamide. Data are mean ± SEM; *P*-values were estimated by one-way ANOVA test in **B** (***P<0.001) and by Student's *t*-test in **C**, **D** (*P<0.05, **P< 0.01).

Figure 5. A) Immunoblot and **B)** densitometry analysis of phospho-Ser1981-ATM (P-ATM), Bcl-xL, Bak, Cytochrome c, and PARP (PARP cleavage) proteins from tumor tissue extracts treated with vehicle (aqueous-PEG, n = 5), enzalutamide (n = 8), PAWI-2 (n = 9) and combination of

JPET Fast Forward. Published on October 3, 2019 as DOI: 10.1124/jpet.119.261040
This article has not been copyedited and formatted. The final version may differ from this version.

enzalutamide and PAWI-2 (n = 5). Tumors excised from mice on day 21 of the study as shown in **Fig. 4**. HSP90 was used as an internal control in **A**; Enza, enzalutamide. Data are mean ± SEM in **B**; *P*-values were estimated by Student's *t*-test (**P*<0.05, ***P*<0.01, ****P*<0.001).

JPET Fast Forward. Published on October 3, 2019 as DOI: 10.1124/jpet.119.261040
This article has not been copyedited and formatted. The final version may differ from this version.

Table 1. Effect of PAWI-2 on PCa cell viability and apoptosis and genomic and expression phenotypes of prostate cancer cell lines used in this study

Cell Lines	**Viability** IC_{50} ± SD, nM (*N*)[a]	**Apoptosis** EC_{50} ± SD, nM (*N*)[a]	***TP53* alleles**[b]	**AR expression**[c]	**Androgen response**[c]
PC-3	18 ± 6 (*8*)	35 ± 5 (*6*)	fs-sc/del	–/low	AI
LNCaP	14 ± 4 (*8*)	11 ± 3 (*6*)	WT/WT	+	AD
PCSD1[d]	60 ± 8 (*3*)		Unknown	Unknown	Unknown

[a]IC_{50} or EC_{50} is the mean ± the standard deviation (SD) of 3-8 independent determinations in the presence of PAWI-2. *N* stands for the number of replicate experiments;
[b]WT, wild-type; *TP53*, human p53 gene; fs-sc, frame shift producing a stop codon; del, allele deletion;
[c]AR, androgen receptor; AD, androgen-dependent growth; AI, androgen-independent growth;
[d]PCSD1 cells were human prostate primary cancer cells freshly isolated from intra-femoral xenografts (Dr. Jamieson, Moores Cancer Center, UCSD)(Raheem et al., 2011; Godebu et al., 2014).

JPET Fast Forward. Published on October 3, 2019 as DOI: 10.1124/jpet.119.261040
This article has not been copyedited and formatted. The final version may differ from this version.

Table 2. Effect of PAWI-2 on PCa cell viability in combination with enzalutamide or abiraterone

Cell Lines	Cell Viability (IC_{50} ± SD, μM) Drug/Combination[a]				
	Enza	Abi	Enza + Abi	Enza + PAWI-2[b]	Abi + PAWI-2[b]
PC-3	>10[c]	>10[c]	>10[c]	1.4 ± 0.6	>10[c]
LNCaP	2.3	6.2	2.5	0.14 ± 0.04	2.7

[a]Enza, enzalutamide; Abi, abiraterone;
[b]Concentration of PAWI-2 was 8 nM in PC-3 cells and 2 nM in LNCaP cells, respectively; <IC_{50}
[c]Compounds were not potent up to 10 μM treated concentration.

JPET Fast Forward. Published on October 3, 2019 as DOI: 10.1124/jpet.119.261040
This article has not been copyedited and formatted. The final version may differ from this version.

Table 3. Summary of combination index (CI) values to quantify synergism. Chou-Talalay analysis of treatment of PAWI-2 with enzalutamide and/or abiraterone in PC-3 and LNCaP PCa cells.

Cell lines	Drug/Combo[a]	CI[b] values at different EDs[c]			
		ED_{50}	ED_{75}	ED_{90}	ED_{95}
PC-3	Enza + Abi	>50	>50	>50	>50
	Enza + PAWI-2	0.97	**0.76**[d]	**0.54**[d]	**0.48**[d]
	Abi + PAWI-2	0.97	0.92	0.92	1.10
	Enza + Abi + PAWI-2	1.30	0.97	**0.72**[d]	**0.58**[d]
LNCaP	Enza + Abi	1.39	1.79	1.97	2.03
	Enza + PAWI-2	**0.76**[d]	**0.37**[d]	**0.19**[d]	**0.13**[d]
	Abi + PAWI-2	**0.78**[d]	**0.74**[d]	**0.72**[d]	**0.70**[d]
	Enza + Abi + PAWI-2	0.92	0.97	1.03	1.08

[a]Enza, enzalutamide; Abi, abiraterone; the ratios of Enza:PAWI-2 and Abi:PAWI-2 were 5:1 and 30:1 in PC-3 cells and 25:1 and 150:1 in LNCaP cells, repectively;
[b]Combination Index, (CI) values were calculated based on the Chou-Talalay method (Chou, 2010); Values of CI < 1, = 1 and > 1 indicate synergism, additive and antagonism, respectively;
[c]$ED_{50,\ 75,\ 90,\ 95}$ represent concentrations that cause 50%, 75%, 90% and 95% of proliferation inhibition, respectively;
[d]Bolded values show synergy.

JPET Fast Forward. Published on October 3, 2019 as DOI: 10.1124/jpet.119.261040
This article has not been copyedited and formatted. The final version may differ from this version.

Figure 1.

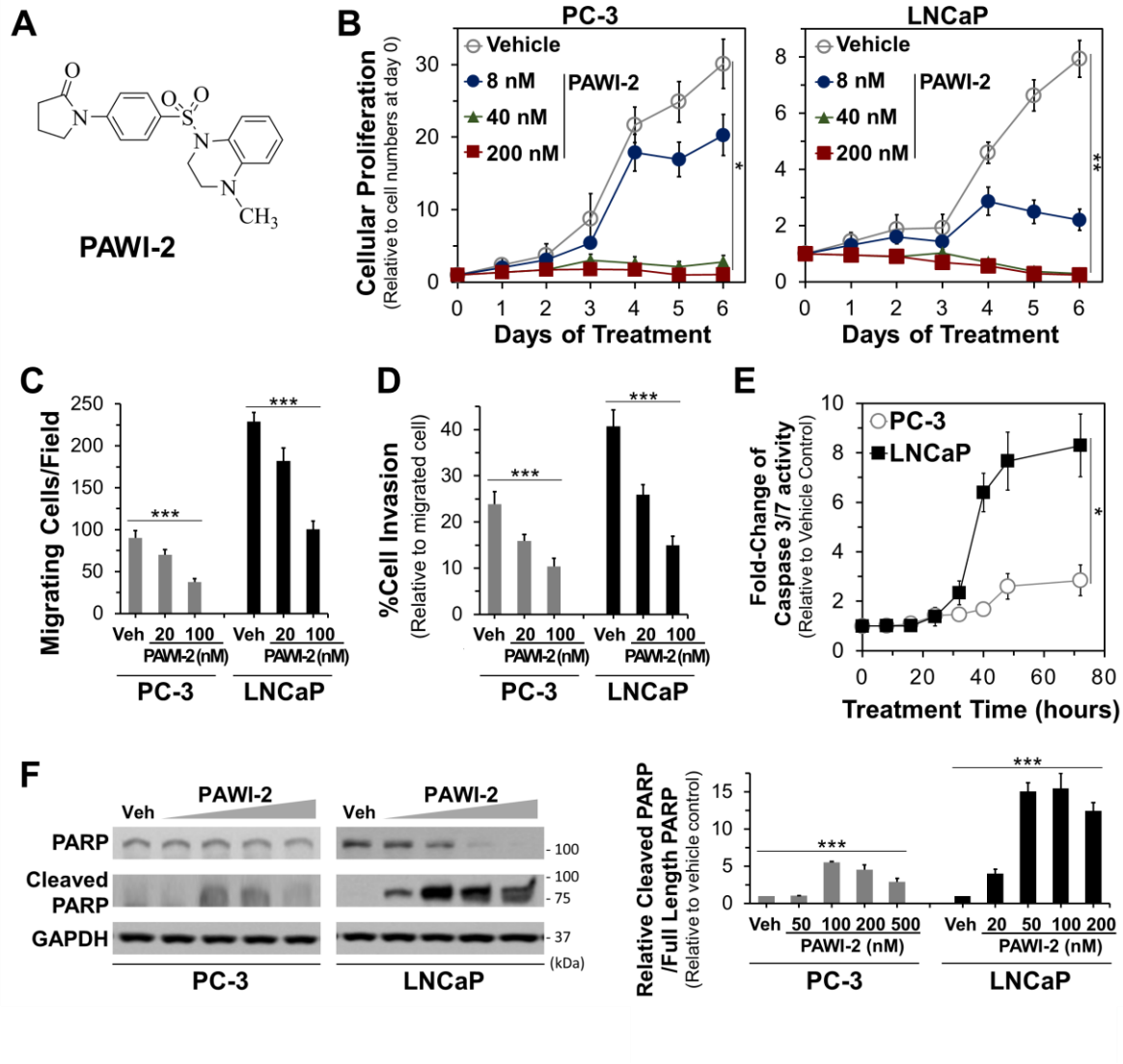

JPET Fast Forward. Published on October 3, 2019 as DOI: 10.1124/jpet.119.261040
This article has not been copyedited and formatted. The final version may differ from this version.

Figure 2.

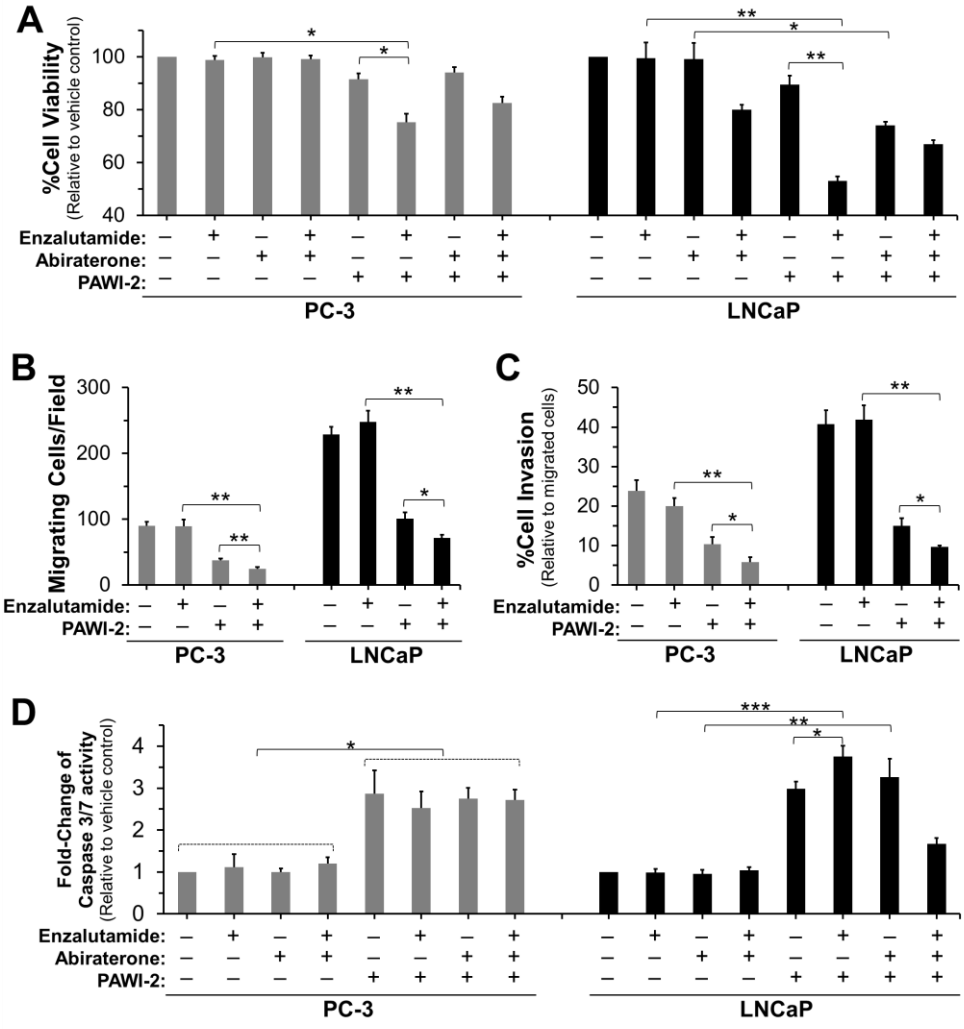

JPET Fast Forward. Published on October 3, 2019 as DOI: 10.1124/jpet.119.261040
This article has not been copyedited and formatted. The final version may differ from this version.

Figure 3.

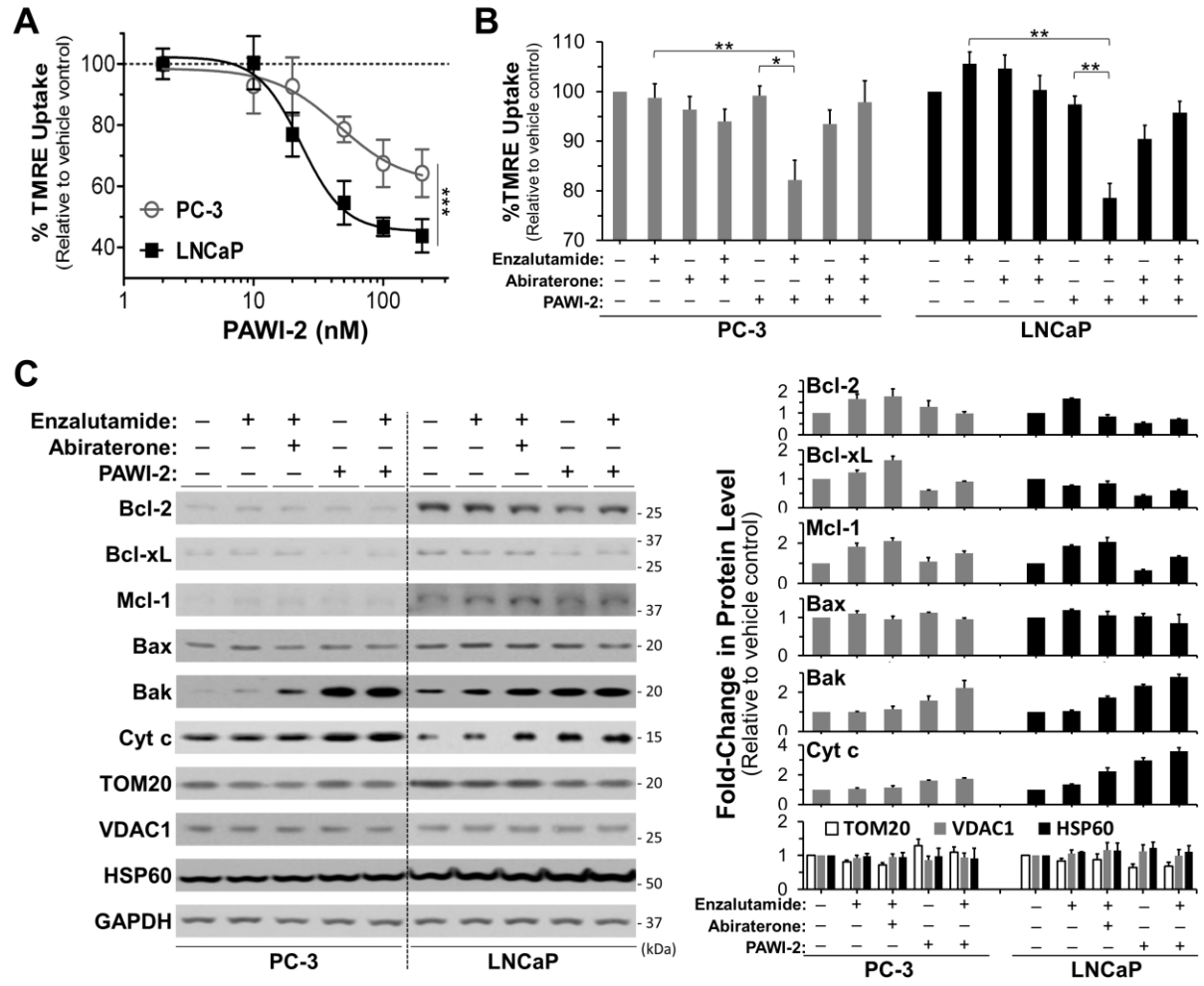

JPET Fast Forward. Published on October 3, 2019 as DOI: 10.1124/jpet.119.261040
This article has not been copyedited and formatted. The final version may differ from this version.

Figure 4.

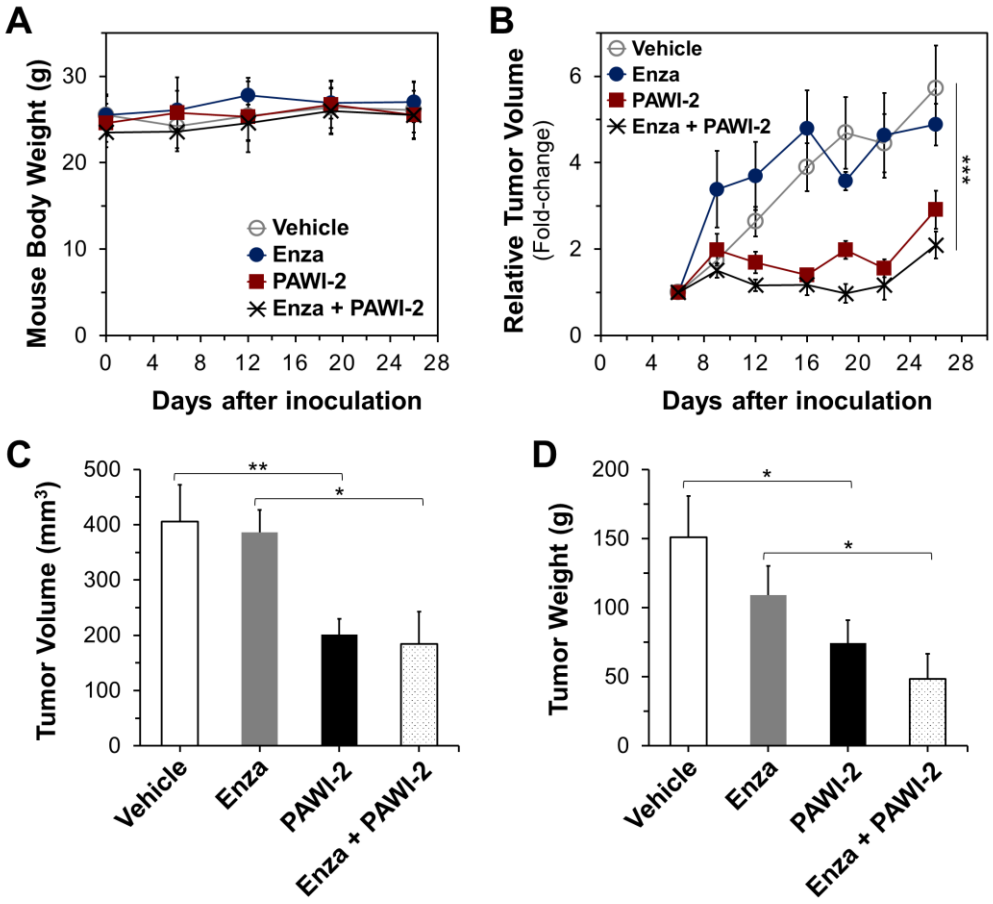

JPET Fast Forward. Published on October 3, 2019 as DOI: 10.1124/jpet.119.261040
This article has not been copyedited and formatted. The final version may differ from this version.

Figure 5.